ON THE GLOBAL DYNAMICS OF A THREE-DIMENSIONAL FORCED-DAMPED DIFFERENTIAL SYSTEM

JAUME LLIBRE[1], Y. PAULINA MARTÍNEZ[2] AND CLÀUDIA VALLS[3]

Abstract. In this paper by using the Poincaré compactification of $\mathbb{R}^3$ we make a global analysis of the model $x' = -ax + y + yz$, $y' = x - ay + bxz$, $z' = cz - bxy$. In particular we give the complete description of its dynamics on the infinity sphere. For $a + c = 0$ or $b = 1$ this system has invariants. For these values of the parameters we provide the global phase portrait of the system in the Poincaré ball. We also describe the α and ω-limit sets of its orbits in the Poincaré ball.

1. Introduction and statement of the main results

We consider the autonomous polynomial differential system

$$\begin{aligned} \dot{x} &= -ax + y + yz, \\ \dot{y} &= x - ay + bxz, \\ \dot{z} &= cz - bxy, \end{aligned} \tag{1}$$

where a, b, c are real parameters and $b > 0$. As usual the dot denotes derivative with respect to the time t. This system was proposed and studied by Pehlivan [9] extending a previous study of Craik and Okamoto [2] including linear forcing and damping. It is a relevant system because it arises in mechanical, electrical and fluid-mechanics (see for instance [7, 8] and the references therein) and can display simultaneously unbounded and chaotic solutions, a non common phenomena in chaotic systems. In this way some important properties are similar to the properties of the well-known Lorenz system (see [6] and the references therein). For instance one can easily check that system (1) is invariant under the change of variables $(x, y, z) \mapsto (-x, -y, z)$ consequently if $(x(t), y(t), z(t))$ is a solution of system (1), then $(-x(t), -y(t), z(t))$, i.e. its symmetric with respect to the z-axis, is also a solution. Moreover, since the divergence of system (1) is $c - 2a$ the phase volume under the flow of system (1) shrinks uniformly if $c - 2a < 0$ (as it happens in the Lorenz system for certain relation on its parameters). Thus in this case the attractor presented by this system has zero Lebesgue

---

2010 *Mathematics Subject Classification.* 34C05, 34C07, 34C08.

Key words and phrases. Global dynamics, Poincaré compactification, forced-damped system, invariant algebraic curve, invariant.

measure (as in the Lorenz system), but both systems are not topologically equivalent, since the number and local stability of their singular points are quite different.

The integrability of system (1) has been studied in [4] where the authors give the description of all the invariant algebraic curves of the system. Let U be an open subset of $\mathbb{R}^3$. A *first integral* $H\colon U \to \mathbb{R}$ of system (1) is a non-locally constant function which is constant on the trajectories of the system.

We say that two C^1 functions $H_1, H_2\colon U \to \mathbb{R}$ are independent on U if the 2×3 matrix $\partial(H_1, H_2)/\partial(x, y, z)$ has rank 2 at all points $(x, y, z) \in U$ except, perhaps, on a subset of zero Lebesgue measure. System (1) is *integrable* if it has two independent first integrals. If a system is integrable then we can obtain its global phase portrait simply by performing the intersection of the level sets of its first integrals.

A function $I(x, y, z, t)$ is an *invariant* of system (1) if $dI/dt = 0$ on the trajectories of the system, that is, an invariant is a first integral which depends on the time. The following result was proved in [4].

Theorem 1. *The following statements hold for system* (1)*.*

(a) *If $c = a = 0$ and $b = 1$, it is completely integrable with the two independent first integrals $H_0 = x^2 + (z + 1)^2$ and $H_1 = x^2 - y^2$.*
(b) *If $b = 1$, $a = 0$ and $c \neq 0$, it has the first integral $H_1 = x^2 - y^2$.*
(c) *If $b = 1$ and $a \neq 0$ it has the invariant $I_1 = H_1 e^{2at} = (x^2 - y^2)e^{2at}$.*
(d) *If $c = -a$ with $a \neq 0$ it has the invariant $I_2 = (b(x^2 - y^2 - z^2) + z^2)e^{2at}$.*

Theorem 1 will be used in the following sections for studying the global dynamics of system (1) having a first integral or an invariant. As any polynomial differential system, system (1) can be extended to an analytic system on a closed ball of radius one, whose interior is diffeomorphic to $\mathbb{R}^3$ and its invariant boundary, a two-dimensional sphere $\mathbb{S}^2$ plays the role of the infinity of $\mathbb{R}^3$. This ball will be denoted by B and called the *Poincaré ball*, due to the fact that the technique for doing so is the Poincaré compactification, which is described in detail in [1] (in fact in that paper is done for $\mathbb{R}^n$).

Two polynomial vector fields are said to be *topologically equivalent* if there exists a homeomorphism on the closed Poincaré ball carrying orbits of the flow induced on the Poincaré ball by the first vector field into orbits of the flow induced in the Poincaré ball by the second vector field preserving or reversing the orientation of all the orbits.

By using this compactification technique for the dynamics of system (1), we can prove the next result.

Theorem 2. *For all values of the parameters $a, b, c \in \mathbb{R}$ with $b > 0$, the phase portrait of system* (1) *on the sphere at infinity, $\mathbb{S}^2$, is topologically* *equivalent to that of Figure 1. In that figure we can see that there exist four centers at the positive and negative endpoints of the x- and y-axis and two hyperbolic saddles at the positive and negative endpoints of the z-axis.*

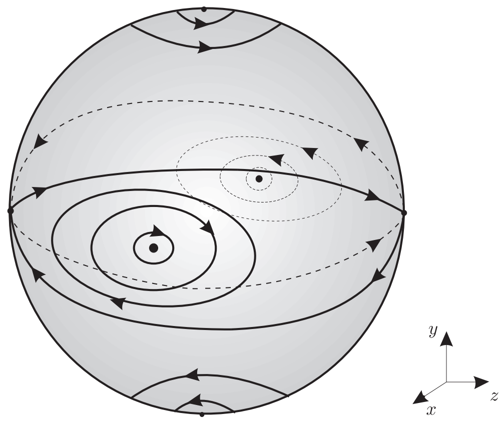

FIGURE 1. Phase portrait of system (1) on the sphere at infinity.

Note that the dynamics at infinity does not depend on the parameter values.

Now we continue the study of the dynamics of system (1) for the values of the parameters in Theorem 1, that is when $b = 1$ or $a + c = 0$ with $a \neq 0$ (and $b \neq 1$). We provide the description of the global dynamics of this polynomial differential system in its compactification on the Poincaré ball and we describe the α- and ω-limit sets of all orbits of system (1) for some values of the parameters.

Theorem 3. *The dynamics of the three-dimensional forced-damped differential system* (1) *in the Poincaré ball under the four assumptions given in the statement of Theorem 1 are described in section 4.*

The paper is organized as follows. In section 2 we summarize several preliminary results of system (1). In section 3 we prove Theorem 2 by means of the Poincaré compactification technique, and in section 4 we prove Theorem 3.

2. Preliminaries

Lemma 4. *If $\phi(t) = (x(t), y(t), v(t))$ is a trajectory of the compactified system* (1) *with $a \neq 0$ and $c = -a$, or $a \neq 0$ and $b = 1$, then its α-limit set $\alpha(\phi)$ and its ω-limit set $\omega(\phi)$ are contained in the closure in the Poincaré ball of the sets $\{H_1 = x^2 - y^2 = 0\}$ when $b = 1$, and $\{H_2 = b(x^2 - y^2 - z^2) + z^2 = 0\}$ when $c = -a \neq 0$ (see Theorem 1)*

Proof. Assume first that $a > 0$. Let $q_1 \in \omega(\phi)$. Then there exists a sequence $\{t_n\}$ such that $t_n \to \infty$ and $\phi(t_n) \to q_1$. Thus, by statements (d) and (e) of Theorem 1 we have

$$H_i(\phi(t_n)) = \frac{\kappa}{e^{2at_n}} \to 0 \quad \text{as } t_n \to \infty,$$

where κ is constant. So $H_i(\phi(t_n)) \to H_i(q_1) \to 0$ as $n \to \infty$. Hence q_1 is in the closure in the Poincaré ball of the set $\{H_i = 0\}$.

Suppose now that $q_2 \in \alpha(\phi)$. Then there exists a sequence $\{t_n\}$ such that $t_n \to -\infty$ and $\phi(t_n) \to q_2$. Hence

$$H_i(\phi(t_n)) \cdot e^{2at_n} \to H_i(q_2) \cdot 0 = \kappa \quad \text{as } t_n \to -\infty.$$

Thus the constant κ is zero and then $H_i(\phi(t_n)) \cdot e^{2at_n} \to 0$. This implies that $H_i(\phi(t_n)) \to 0$ and so q_2 is in the closure in the Poincaré ball of the set $\{H_i = 0\}$.

The case $a < 0$ can be done in the same manner reverting the roles of q_1 and q_2. □

Lemma 5. *For all values of the parameters a, b, c the z-axis is an invariant set of system* (1)*. The flow restricted to this invariant straight line is as follows: if $c < 0$ the origin $(0, 0, 0)$ is a global attractor. If $c > 0$ then the origin is a global repeller. If $c = 0$ all points in the z-axis are singular.*

Proof. It follows directly from system (1). □

Now we study the finite singular points whenever $a \neq 0$ and $c = -a$ or $ac \neq 0$ and $b = 1$. Let p be a hyperbolic singular point of system (1) whose Jacobian matrix has k eigenvalues with negative real part. Then its *stability index* is k. Of course, $0 \leq k \leq 3$. The topology index of p is given by $(-1)^k$ (see Theorem 8.1 of [5]).

Lemma 6. *Consider system* (1) *with $b = 1$ and $ac \neq 0$.*

(i) *If $c < 0$ and $a > 1$ the unique singular point is the origin which has stability index* 3 *(an attractor).*
(ii) *If $c < 0$ and $a = 1$ the unique singular point is the origin whose eigenvalues of its Jacobian matrix are $-2, 0, c$.*
(iii) *If $c < 0$ and $a \in (-1, 1)$ it has three singular points: the origin and $R^0_\pm = (\pm\sqrt{c(a-1)}, \pm\sqrt{c(a-1)}, a-1)$. The origin has stability index one and the points $R^0_\pm$ both have stability index two if $a < 0$ and stability index three if $a > 0$.*
(iv) *If $c < 0$ and $a = -1$ it has three singular points: the origin whose eigenvalues of its Jacobian matrix are $2, 0, c$, and the two points $(\pm\sqrt{-2c}, \pm\sqrt{-2c}, -2)$ which both have stability index two.*
(v) *If $c < 0$ and $a < -1$ it has five singular points: the origin which has stability index 1, $R^0_\pm$ given in statement (iii) which have both stability*

index 1, and $R^1_\pm = (\mp\sqrt{c(a+1)}, \pm\sqrt{c(a+1)}, -a-1)$ *which have both stability index two.*

(vi) *If* $c > 0$ *and* $a > 1$ *it has five singular points which are the origin (with stability index two),* $R^0_\pm$ *and* $R^1_\pm$ *having the four of them stability index one.*

(vii) *If* $c > 0$ *and* $a = 1$ *it has two singular points which are the origin (whose eigenvalues of its Jacobian matrix are* $(-2, 0, c)$ *and* $(\pm\sqrt{2c}, \mp\sqrt{2c}, -2)$ *which have both stability index one.*

(viii) *If* $c > 0$ *and* $a \in (-1, 1)$ *it has three singular points which are the origin and* $R^1_\pm$ *and all of them have stability index one.*

(ix) *If* $c > 0$ *and* $a = -1$ *it has the origin as its unique singular point whose eigenvalues of its Jacobian matrix are* $2, 0, c$.

(x) *If* $c > 0$ *and* $a < -1$ *it has the origin as its unique singular point which has stability index zero (a repeller).*

Proof. The proof of the lemma follows by direct calculations. □

Lemma 7. *Consider system* (1) *with* $c = -a$, $a \neq 0$ *and* $b \neq 1$*:*

(i) *If* $a > 1$ *it has the origin as its unique singular point which has stability index three (an attractor).*

(ii) *If* $a = 1$ *it has the origin as its unique singular point whose eigenvalues of its Jacobian matrix are* $-2, -1, 0$.

(iii) *If* $a \in (-1, 1)$ *it has three singular points which are the origin and*

$$S_\pm = \left(\pm B, \pm\frac{(-1+b-A)B}{2a}, \frac{-1-b+A}{2b}\right)$$

with

$$A = \sqrt{1 + b(b + 4a^2 - 2)}, \quad B = \sqrt{\frac{-1 - b(2a^2 - 1) + A}{2b^3}}.$$

All three points have stability index two when $a \in (0, 1)$ *and stability index one when* $a \in (-1, 0)$.

(iv) *If* $a = -1$ *it has the origin as its unique singular point whose eigenvalues of its Jacobian matrix are* $2, 1, 0$.

(v) *If* $a < -1$ *it has the origin as its unique singular point which has stability index zero (a repeller).*

Proof. The proof of the lemma follows by direct computations. □

3. Proof of Theorem 2

For studying the infinity of the Poincaré ball B we analyze the flow at infinity for the local charts U_1, U_2 and U_3 (see [1]), as well as in the local charts V_1, V_2 and V_3.

3.1. **Study of the infinity in the local charts U_1 and V_1.** The Poincaré compactification $p(X)$ of system (1) in the local chart U_1 is given by

$$\begin{aligned}\dot z_1 &= bz_2 + z_3 - z_1^2 z_2 - z_1^2 z_3,\\ \dot z_2 &= -bz_1(a+c)z_2z_3 - z_1z_2^2 + -z_1z_2z_3,\\ \dot z_3 &= az_3^2 - z_1z_2z_3 - z_1z_3^2.\end{aligned} \tag{2}$$

Note that the unique singular point of system (2) on $z_3 = 0$ is the origin $(0,0,0)$ and the eigenvalues of the linear part of the system at this point are $\pm ib$, and 0. System (2) restricted to $z_3 = 0$ (because this corresponds to the sphere at infinity) reduces to

$$\dot z_1 = bz_2 - z_1^2 z_2, \quad \dot z_2 = -bz_1 - z_1 z_2^2, \tag{3}$$

which has $(0,0)$ as its unique singular point. The eigenvalues of the linear part of the system at this point are $\pm i\sqrt{b}$. Hence the point is either a focus or a center. Since system (3) has the first integral $H = (z_1^2 - b)/(b + z_2^2)$, the origin is a center. Using this first integral and observing that system (3) has $z_1 = \pm\sqrt{b}$ as invariant straight lines, it follows that the phase portrait on the local chart U_1 on the infinite sphere is as shown in Figure 2. The flow on the local chart V_1 is the same than the flow of U_1 reversing the time, because the compactified vector field $p(x)$ in V_1 coincides with the vector field $p(X)$ in U_1 multiplied by -1 (see again [1]).

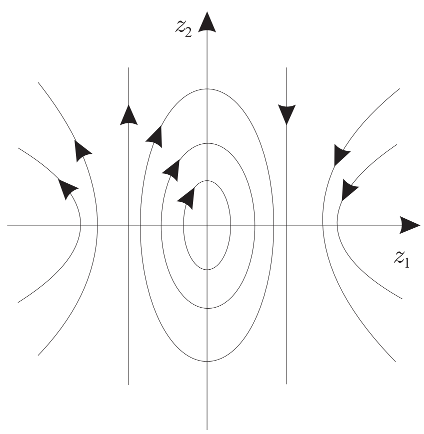

FIGURE 2. Phase portrait of system (3).

3.2. **Study of the infinity in the local charts U_2 and V_2.** The expression of the Poincaré compactification in the local chart U_2 of system (1) writes as

$$\begin{aligned}\dot z_1 &= z_2 - bz_1^2 z_2 + z_3 - z_1^2 z_3,\\ \dot z_2 &= -bz_1 - bz_1z_2^2 + az_2z_3 + cz_2z_3 - z_1z_2z_3,\\ \dot z_3 &= -bz_1z_2z_3 + az_3^2 - z_1z_3^2,\end{aligned} \tag{4}$$

Taking $z_3 = 0$, system (4) becomes

$$\dot{z}_1 = z_2 - bz_1^2 z_2, \quad \dot{z}_2 = -bz_1 - bz_1 z_2^2 \tag{5}$$

which has $(0,0)$ as its unique singular point with eigenvalues $\pm i\sqrt{b}$. System (5) has the first integral $H = (bz_1^2 - 1)/(1 + z_2^2)$. Hence the origin in the local chart U_2 restricted to the infinite sphere is a center. Using the first integral and observing that system (5) has $z_1 = \pm\sqrt{b}$ as invariant lines it follows that the phase portrait on the local chart U_2 over the infinite sphere is again the one shown in Figure 2.

Again we observe that the flow on the local chart V_2 is the same as the flow on the local chart U_2 reversing the time, because the compactified vector field $p(X)$ in V_2 coincides with the vector field $p(X)$ in U_2 multiplied by -1.

3.3. **Study of the infinity in the local charts U_3 and V_3.** The expression of the Poincaré compactification of system (1) in the local chart U_3 is given by

$$\begin{aligned} \dot{z}_1 &= z_2 + bz_1^2 z_2 - az_1 z_3 - cz_1 z_3 + z_2 z_3, \\ \dot{z}_2 &= bz_1 + bz_1 z_2^2 + z_1 z_3 - az_2 z_3 - cz_2 z_3, \\ \dot{z}_3 &= bz_1 z_2 z_3 - cz_3^2. \end{aligned} \tag{6}$$

If $z_3 = 0$ the unique singular point of system (6) is $p = (0,0,0)$. We want to study the local flow of this system around p. The eigenvalues of the linear part at p are $\pm\sqrt{b}$ and 0. Hence, system (6) has a saddle at p when we restrict the system to the infinity (that is to $z_3 = 0$ which is invariant) and a one-dimensional center manifold at p contained in the interior of the ball diffeomorphic to $\mathbb{R}^3$. Note that if we consider $z_1 = z_2 = 0$ then system (6) reduces to $\dot{z}_1 = 0$, $\dot{z}_2 = 0$ and $\dot{z}_3 = -cz_3^2$. So there exists a trajectory of system (1) which escapes to infinity as $t \to \pm\infty$ (depending on the sign of c). In fact since the infinity of system (1) in the local chart U_3 is invariant, the unique way in order that a solution reaches the infinity is tending to the singular point p (a saddle at the sphere at infinity) and this is possible only over the center manifold $z_1 = z_2 = 0$. In the local chart V_3 we have to change the sign of system (6) because the compactified vector field $p(X)$ in V_3 is the same as in U_3 multiplied by -1. So in V_3 the dynamics on the z_3-axis is governed by the equation $\dot{z}_3 = cz_3^2$.

Proof of Theorem 2. Considering the analysis made in the previous subsections we obtain the phase portrait of system (1) on the sphere at infinity: the system has four centers, localized at the endpoints of the x and y-axis, and two saddles localized at the endpoints of the z-axis (see Figure 1). Moreover, the orbits of the system may come and go to infinity along a one-dimensional center manifold of these saddle points, depending on the sign of the parameter c. The dynamics near the center at infinity is more complex, due to the periodic orbits. □

4. Proof of Theorem 3

In this section we prove Theorem 3. We consider the invariants and first integrals given in Theorem 1 and how the surfaces end in the Poincaré sphere at infinity.

4.1. Case $b = 1$, $a = c = 0$.

In this case system (1) is completely integrable. There are three straight lines filled of singularities $(0, 0, z)$, $(x, 0, -1)$ and $(0, y, -1)$. The endpoints of the straight line $(0, 0, z)$ on the Poincaré sphere are $(0, 0, \pm 1)$, the endpoints of the straight line $(x, 0, 1)$ are $(\pm 1, 0, 0)$, and the endpoints of the straight line $(0, y, -1)$ are $(0, \pm 1, 0)$. According to the introduction the trajectories are in the intersection of the elliptic cylinder $x^2 + (z + 1)^2 = c_1$ with the hyperbolic cylinder $x^2 - y^2 = c_2$, where $c_1 \geq 0$ and $c_2 \in \mathbb{R}$. The intersection produces families of periodic orbits, and for $c_1 = c_2$ the intersection occurs on the straight line $(x, 0, -1)$.

4.2. Case $b = 1$, $a = 0$, $c \neq 0$.

In this case $H_1 = x^2 - y^2$ is a first integral. We study the dynamics of system (1) restricted to the hyperbolic cylinders $x^2 - y^2 = \pm r^2$ if $r \neq 0$, and on the planes $(x - y)(x + y) = 0$ for $r = 0$.

For $r = 0$ the level is formed by two invariant planes with endpoints being the separatrices of the saddles on the Poincaré sphere. In the plane $y = -x$ system (1) becomes

$$\dot{x} = -x(1 + z), \quad \dot{z} = cz + x^2. \tag{7}$$

If $c < 0$ the unique singular point of system (7) is the origin $(0, 0)$ which is a stable node.

Now we study the phase portrait in a neighborhood of the infinity. Since system (7) is defined in $\mathbb{R}^2$ we study it doing the Poincaré compactification in the Poincaré disc, see for more details on the Poincaré disc, Chapter 5 of [3]. System (7) in the local chart U_1 given by the Poincaré compactification is

$$z_1' = 1 + z_1(z_1 + z_2 + cz_2), \quad z_2' = z_2(z_1 + z_2).$$

Note that there are no infinite singular points on U_1. On the other hand system (7) on the local chart U_2 is

$$z_1' = -z_1(1 + z_1^2 + z_2 + cz_2), \quad z_2' = -z_2(z_1^2 + cz_2).$$

We study the origin of U_2 which is a semi-hyperbolic singular point. Applying Theorem 2.19 of [3] we get that it is a saddle-node with central manifold on $z_1 = 0$ (where the flow is increasing), and the stable separatrices are located on $z_2 = 0$. Since system (7) has degree two, the local phase portrait on V_2 have the opposite stability.

Since the unique finite singular point of system (7) is the origin and the straight line $x = 0$ is invariant, the system has no limit cycles. In short, by the Poincaré-Bendixson theorem (see for instance Corollary 1.30 of [3]) the unstable separatrix of the saddle-node at the origin of U_2 has ω-limit the finite singular point $(0,0)$. See the phase portrait in the Poincaré disc of Figure 3(a).

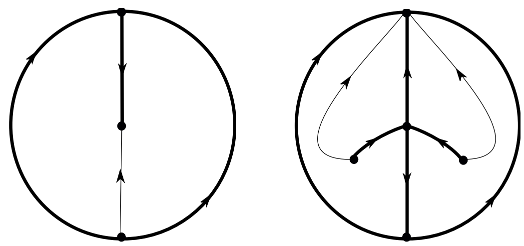

(a) (b)

FIGURE 3. Global phase portrait of system (7) for $b = 1$ and $a = 0$. (a): with $c < 0$, (b): with $c > 0$.

If $c > 0$ there are two more singular points beyond the origin. The origin is a saddle in this case and the two new singular points are unstable nodes if $c - 8 \geq 0$, or unstable foci if $c - 8 < 0$. Proceeding in a similar way to the case $c < 0$, the unique infinite singular points are the origins of U_2 and V_2, which are saddle-nodes, but now the nodal part of the saddle-node is in U_2, see Figure 3(b). The unstable separatrices of the origin are contained in the straight line $x = 0$ and they go to the origins of U_2 and V_2. By the Poincaré-Bendixson theorem the stable separatrices at the origin have α-limit at the repeller nodes (or foci) in the finite region. This completes the global phase portrait of system (7) for $c > 0$, see Figure 3(b).

In the plane $y = x$ system (1) becomes

$$\dot{x} = x(1+z), \quad \dot{z} = cz - x^2. \tag{8}$$

Note that system (8) is the same as system (7) doing the reparameterization of the time $t \to -t$ and changing the parameter c by $-c$. This implies that the global phase portraits of system (8) are topologically equivalent to the ones shown in Figure 3.

The straight line $(0,0,z)$ (intersection of the planes $y = -x$ and $y = x$) is invariant with its points having $(0,0,0)$ as their ω-limit.

For $r \neq 0$ we have a pair of hyperbolic cylinders. System (1) restricted to the hyperbolic cylinder $x^2 - y^2 = r^2$, $r \neq 0$, (taking $x = \pm\sqrt{r^2 + y^2}$) is, respectively

$$\dot{y} = \sqrt{r^2 + y^2}(1+z), \quad \dot{z} = cz - y\sqrt{r^2 + y^2}, \tag{9}$$

and

$$\dot{y} = -\sqrt{r^2 + y^2}(1+z), \quad \dot{z} = cz + y\sqrt{r^2 + y^2}. \tag{10}$$

Note that system (9) and system (10) are the same doing the change $c \to -c$ and reparameterizing the time by $t \to -t$. Then it is sufficient to analyse the phase portraits of system (9).

System (9) has a unique finite singular point which is a stable node or stable focus if $c < 0$, and an unstable node or unstable focus if $c > 0$.

There are no infinite singular points in the local chart U_1. In the local chart U_2 system (9) becomes

$$z_1' = -cz_1z_2 + (1 + z_1^2 + z_2)\sqrt{z_1^2 + r^2z_2^2}, \quad z_2' = -z_2\left(cz_2 - z_1\sqrt{z_1^2 + r^2z_2^2}\right). \tag{11}$$

The origin of system (11) is an infinite singular point whose eigenvalues are 0 and 1. Since it is semi-hyperbolic it can be a saddle, a node or a saddle-node. Considering that the sum of the indices of all singular points on the Poincaré sphere is 2 by the Poincaré-Hopf Theorem (see Theorem 6.30 of [3]), and since the finite singular points are two nodes (or two foci), it holds that the origin in U_2 must be a saddle-node. From (11) we have $z_2'|_{z_1=0} = -cz_2^2$ and then the saddle-node at the origin of U_2 has its unstable separatrix on the z_1-axis. Furthermore for $c > 0$ the flow is increasing on the z_2-axis and for $c < 0$ it is decreasing on the z_2-axis.

Doing the change of time $d\tau = \sqrt{r^2 + y^2}\,dt$ system (9) becomes

$$\dot{y} = 1 + z, \quad \dot{z} = \frac{c}{\sqrt{r^2 + y^2}}z - y.$$

Since the divergence of this system is $c/\sqrt{r^2 + y^2} \neq 0$, system (9) has no limit cycles due to the Bendixson criterion, see for instance Theorem 7.10 of [3].

Note that by the Poincaré-Bendixson theorem the unstable separatrix coming from the origin of U_2 must go to the finite attractor. In summary, the global phase portrait for $c > 0$ (for $c < 0$ is the same reversing the direction of the orbits) is the one of Figure 4.

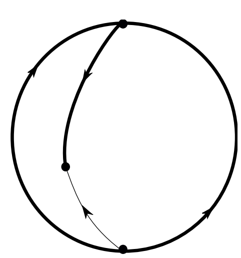

FIGURE 4. Global phase portrait of system (9).

Furthermore system (1) restricted to the hyperbolic cylinder $x^2 - y^2 = -r^2$, $r \neq 0$, (taking $y = \pm\sqrt{r^2 + x^2}$) is, respectively

$$\dot{x} = \sqrt{r^2 + x^2}(1 + z), \quad \dot{z} = cz - x\sqrt{r^2 + x^2}, \tag{12}$$

and

$$\dot{x} = -\sqrt{r^2 + x^2}(1 + z), \quad \dot{z} = cz + x\sqrt{r^2 + x^2}. \tag{13}$$

Systems (12) and (13) coincide with systems (9) and (10), respectively, doing the change of variables $(y, z) \to (x, z)$. Then their phase portraits are the same than the one of Figure 4.

The phase portraits in the Poincaré ball for this case can be obtained using the previous information together with Figure 1.

4.3. **Case $b = 1$, $a \neq 0$.** The planes $x = \pm y$ are invariant by the flow of system (1). The boundary at infinity of the invariant planes $y = \pm x$ coincide exactly with the heteroclinic cycles of the saddles at infinity.

Taking $y = x$ system (1) becomes

$$\dot{x} = x(1 - a + z), \quad \dot{z} = cz - x^2. \tag{14}$$

The infinite singular points of system (14) are the same than the infinite singular points of system (7).

If $c = 0$, system (14) has the z-axis filled of singular points. The linear part of the system at the singular points $(0, z)$ has the trivial eigenvalues 0 and $z + 1 - a$. Now by a simple integration of the orbits we get that the orbits of system (14) are contained in the ellipses given by the equation

$$\frac{x^2}{2} + \frac{z^2}{2} + (1 - a)z = d \quad \text{with } d \in \mathbb{R}.$$

See the phase portraits in the Poincaré disc of system (14) with $c = 0$ in Figure 5(a).

If $c \neq 0$ and $c(a - 1) < 0$ the unique singular point of system (14) is the origin $(0, 0)$. If $a - 1 > 0$ it is a stable node, and if $a - 1 < 0$ it is an unstable node, see the phase portraits in Figures 5(b) and 5(c).

If $c \neq 0$ and $a = 1$ the unique singular point is the origin which is a semi-hyperbolic node (stable if $c < 0$ and unstable if $c > 0$), see the phase portraits in Figures 5(b) and 5(c).

If $c \neq 0$ and $c(a - 1) > 0$ there are two more singular points beyond the origin. The origin is a saddle and the two new singular points are nodes if $c(c + 8(1 - a)) \geq 0$ (stable if $c < 0$ and unstable if $c > 0$), or two foci if $c(c + 8(1 - a)) < 0$ (stable if $c < 0$ and unstable if $c > 0$), see the phase portraits in Figures 5(d) and 5(e).

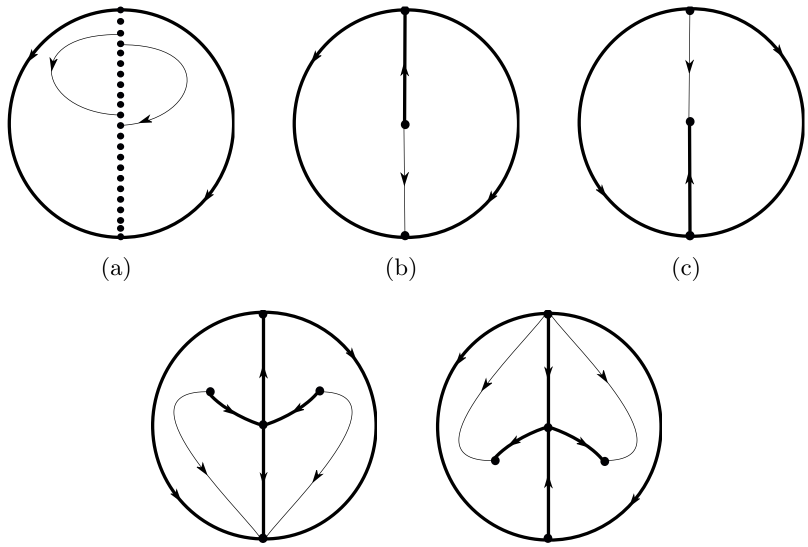

FIGURE 5. Global phase portrait of system (14) with $a \neq 0$. (a): for $c = 0$, (b): for $c > 0$, $(a-1) \leq 0$, (c): for$c < 0$, $(a-1) \geq 0$, (d): for $c > 0$, $(a-1) > 0$, (e): for $c < 0$, $(a-1) < 0$.

Now we perform the analysis on $y = -x$. System (1) becomes

$$\dot{x} = -x(1 + a + z), \quad \dot{z} = cz + x^2. \tag{15}$$

System (15) coincides with system (14) doing a reparametrization of the time $t \to -t$ and changing the parameters $(a, c) \to (-a, -c)$. Then the phase portraits of system (15) are topologically equivalent to the ones shown in Figure 5.

Note that in view of Lemma 6 system (1) under the assumptions of this case can have either two more singular points beyond the origin or four more singular points beyond the origin, two of them located in the plane $x = y$ and the other two on the plane $x = -y$ which are either foci or nodes. Moreover, according to Lemma 4 the ω- and α-limit sets of any point not belonging to the planes $y = \pm x$ are contained in the closure of these planes inside the Poincaré ball.

4.4. **Case** $c = -a$**,** $a \neq 0$**,** $b \neq 1$**.** We will distinguish between the cases $b > 1$ and $0 < b < 1$ (recall that the case $b = 1$ is been considered in subsection 4.3 and that $b > 0$). We consider two cases.

Assume first that $b > 1$. In this case the cone $x^2 - y^2 - (b-1)z^2/b = 0$ is an invariant algebraic surface. System (1) restricted to this cone becomes

either
(16)
$$\dot y = -ay + (1+bz)\sqrt{y^2+(b-1)z^2/b}, \quad \dot z = -az - by\sqrt{y^2+(b-1)z^2/b},$$
or
(17)
$$\dot y = -ay - (1+bz)\sqrt{y^2+(b-1)z^2/b}, \quad \dot z = -az + by\sqrt{y^2+(b-1)z^2/b},$$

Note that system (17) is the same as system (16) with a reparameterization of the time $t \mapsto -t$ and the parameter a interchanged by $-a$. So, the behavior is the same with the stability interchanged and the values of a also changed to $-a$. Hence, we will study only system (16).

If $|a| \geq 1$ the unique singular point of system (16) is the origin. If $a \in (-1,1)$ among the origin there is one more singular point which is
$$S = \Big(\sqrt{\frac{1-2a^2-b+A}{2b}}, \frac{A-1-b}{2b}\Big), \quad A = \sqrt{1+b(4a^2+b-2)}.$$
The eigenvalues of the Jacobian matrix at S are
$$\frac{1}{4\sqrt{b(b-1-2a^2b+A)}}(-b\alpha_1 \pm 2\sqrt{\alpha_2})$$
with
$$\alpha_1 = \sqrt{\frac{1-2a^2-b+A}{b}}(b-1+A) + 4ab\sqrt{\frac{b-1-2a^2b+A}{b^3}}$$
and
$$\alpha_2 = -4+8b-21a^2b-4b^2+9a^2b^2-18a^4b^2-4a^2b^3+A(4-4b+13a^2b+4a^2b^2).$$
We note that $\alpha_1 = 0$ if and only if $a=0$ which is not possible. Hence, if $\alpha_2 \geq 0$ it is a node (stable if $a>0$ and unstable if $a<0$), and if $\alpha_2 < 0$ it is a focus (stable if $a>0$ and unstable if $a<0$).

Now we study the local phase portraits at the origin of system (16). To do so we consider polar coordinates $y = r\cos\theta$, $z = r\sin\theta$ and system (16) becomes

$$\begin{aligned} \dot r &= r\Big(-a + \frac{\cos\theta\sqrt{2b-1+\cos(2\theta)}}{\sqrt{2b}}\Big), \\ \dot\theta &= -\frac{\sqrt{2b-1+\cos(2\theta)}(br+\sin\theta)}{\sqrt{2b}}. \end{aligned} \tag{18}$$

Clearly the origin corresponds to $r=0$ which is invariant under the flow of system (18). On $r=0$, taking into account that $b>1$, we have two singular points which are $\theta=0$ and $\theta=\pi$. Computing the eigenvalues of the Jacobian matrix at these points we get that $(0,0)$ is a saddle if $a<1$ and a stable node if $a \geq 1$ (when $a=1$ this node is semi-hyperbolic). On the other hand the singular point $(0,\pi)$ is a saddle if $a>-1$ and an unstable node if $a \leq -1$ (when $a=-1$ the node is semi-hyperbolic). To obtain the behavior of the origin of system (18) we identify $\theta = 0$ and $\theta = 2\pi$ and $r = 0$ becomes a circle in the cylinder $(r, \theta) \in \mathbb{R} \times \mathbb{S}^1$. In this case the semi-cylinder $r > 0$ corresponds to the plane (x, y) of system (18) around the origin. So we are only interested in the separatrices (or dynamics) of system (18) in $r > 0$. Going back through the change of variables to obtain the local behavior at the origin, we need to shrink the circle to a point. This will be done for the different values of a. More precisely, when $a \leq -1$ we have the phase portrait in Figure 6(a) with $r = 0$ as a circle. Shrinking the circle to a point we conclude that the origin is an unstable node, see Figure 6(b). When $a \in (-1, 0) \cup (0, 1)$ we have the phase portrait in Figure 7(a) again with $r = 0$ as a circle. Going back through the change of variables we get that the origin is formed by two hyperbolic sectors, see Figure 7(b). Finally, when $a \geq 1$ we have the phase portrait in Figure 8(a) with $r = 0$ as a circle. Shrinking the circle to a point we conclude that the origin is a stable node, see Figure 8(b). This concludes the study of the finite singular points of system (16).

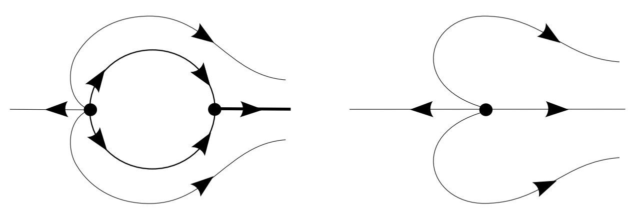

(a) (b)

FIGURE 6. Here $b > 1$ and $a \leq -1$ (a): Local phase portrait at $r = 0$ of system (18), (b): Local phase portrait at the origin of system (16).

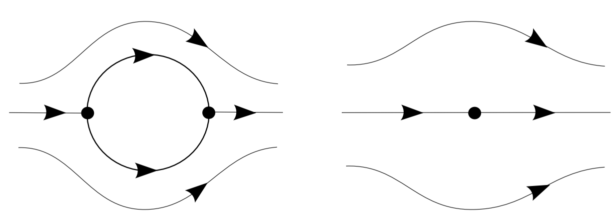

(a) (b)

FIGURE 7. Here $b > 1$ and $a \in (-1, 0) \cup (0, 1)$. (a): Local phase portrait at $r = 0$ of system (18), (b): Local phase portrait at the origin of system (16).

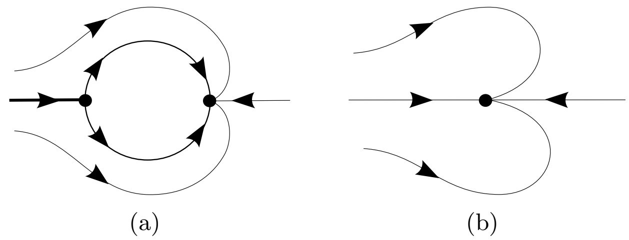

FIGURE 8. Here $b > 1$ and $a \geq 1$. (a): Local phase portrait at $r = 0$ of system (18), (b): Local phase portrait at the origin of system (16).

In the local chart U_1 system (16) writes as

$$
\begin{aligned}
z_1' &= -\sqrt{\frac{(b-1)z_1^2}{b}+1}\left(bz_1^2+b+z_1z_2\right), \\
z_2' &= z_2\left(az_2+\sqrt{\frac{b+(b-1)z_1^2}{b}}(-bz_1-z_2)\right).
\end{aligned}
\tag{19}
$$

Since $b > 1$ system (19) has no infinite singular points. On the other hand system (16) in the local chart U_2 becomes

$$
z_1' = \frac{\sqrt{-1+b+bz_1^2}}{\sqrt{b}}(b+bz_1^2+z_2), \quad z_2' = z_2(\sqrt{b}z_1\sqrt{-1+b+bz_1^2}+az_2).
\tag{20}
$$

Note that the origin of U_2 is not a singular point. So the circle at infinity is a periodic solution.

Doing the rescaling of the time $d\tau = \sqrt{y^2+(b-1)z^2/b}\,dt$, system (16) becomes

$$
\dot{y} = -\frac{a}{\sqrt{y^2+(b-1)z^2/b}}y+1+bz, \quad \dot{z} = -\frac{a}{\sqrt{y^2+(b-1)z^2/b}}z-by.
$$

Since the divergence of this system is $-a/\sqrt{y^2+(b-1)z^2/b} \neq 0$, system (16) has no limit cycles. By the Poincaré-Bendixson theorem we get that their phase portraits in the Poincaré disc are given in Figures 9(a) and 9(b).

According to Lemma 4 for any trajectory γ not starting on the cone we have that $\omega(\gamma)$ and $\alpha(\gamma)$ are contained in the closure of the cone inside the Poincaré ball.

Assume now that $0 < b < 1$. Again the cone $x^2 - y^2 + (1-b)z^2/b = 0$ is an invariant algebraic surface. System (1) restricted to this cone becomes either

$$
\dot{x} = -ax+(1+z)\sqrt{x^2+(1-b)z^2/b}, \quad \dot{z} = -az-bx\sqrt{x^2+(1-b)z^2/b}
\tag{21}
$$

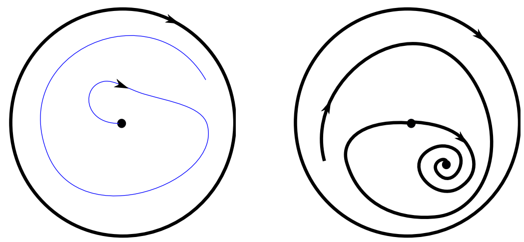

(a) (b)

FIGURE 9. Global phase portraits of system (16) with $b > 1$ and $a \neq 0$. (a): for $|a| \geq 1$, (b): $a \in (-1, 0) \cup (0, 1)$.

or

$$\dot{x} = -ax - (1+z)\sqrt{x^2 + (1-b)z^2/b}, \quad \dot{z} = -az + bx\sqrt{x^2 + (1-b)z^2/b} \tag{22}$$

Note that system (22) is the same as system (21) with a reparameterization of the time $t \mapsto -t$ and the parameter a interchanged by $-a$. So the behavior is the same with the stability interchanged and the values of a also changed to $-a$. Hence, we will study only system (21). However, the study of system (21) can be done in an analogous way to system (16), obtaining the phase portraits of Figure 9. Again, according to Lemma 4 for any trajectory γ not starting on the cone we have that $\omega(\gamma)$ and $\alpha(\gamma)$ are contained in the closure of the cone inside the Poincaré ball.

Acknowledgements

The first author is supported by the Ministerio de Economía, Industria y Competitividad - Agencia Estatal de Investigación grant MTM2016-77278-P (FEDER), the Agència de Gestió d'Ajuts Universitaris i de Recerca grant 2017 SGR 1617, and the European project Dynamics- H2020-MSCA-RISE-2017-777911. The second author is supported by CONICYT PCHA / Postdoctorado en el extranjero Becas Chile / 2018 - 74190062. The third author is partially supported by FCT/Portugal through UID/MAT/04459/2013.

References

[1] A. Cima and J. Llibre, *Bounded polynomial systems*, Trans. Amer. Math. Soc. **318** (1990), 557–579.
[2] A. Craig and H. Okamoto, *A three-dimensional autontomous system with unbounded bending solutions*, Physica D **164** (2002), 168–186.
[3] F. Dumortier, J. Llibre and J.C. Artés, *Qualitative theory of planar differential systems*, Universitext, Spring-Verlag, 2006.
[4] J. Llibre, R. Oliveira and C. Valls *On the DArboux integrability of a three-dimensional forced-damped differential system* J. Nonlinear Math. Phys. **24** (2017), 473–494.
[5] N.G. Lloyd, *Degree Theory*, Cambridge University Press, 1978.

[6] E.N. Lorenz, *Deterministic nonperiodic flow*, J. Atmos. Sci. **20** (1963), 130–141.

[7] T. Miyaji, H. Okamotot and A. Craig, *A Four-Leaf chaotic attractor of a three-dimensional dyamical system*, Internat. J. Bifur. Chaos. Appl. Sci. Engrg. **25** (2015), 1530003, pp. 21

[8] T. Miyaji, H. Okamotot and A. Craig, *Three-dimensional forced-damped dynamical system with rich dynamics: Bifurcations, chaos and unbounded solutions*, Physica D **311-312** (2015), 25–36.

[9] I.Pehlivan, *Four-scroll stellate new chaotic system*, Optoelectronics and Advanced materials–rapid communications **5** (2011), 1003–1006.

[1] Departament de Matemàtiques, Universitat Autònoma de Barcelona, 08193 Bellaterra, Barcelona, Catalonia, Spain

Email address: `jllibre@mat.uab.cat`

[2] Centre de Recerca Matemática, 08193 Bellaterra, Barcelona, Catalonia, Spain

Email address: `yohanna.martinez@uab.cat`

[3] Departamento de Matemática, Instituto Superior Técnico, Universidade Técnica de Lisboa, Av. Rovisco Pais 1049–001, Lisboa, Portugal

Email address: `cvalls@math.ist.utl.pt`